

A new mechanism for ocean-atmosphere
coupling in midlatitudes

A. Czaja, and N. Blunt

Department of Physics, Imperial College, London *

February 22, 2011

Keywords: convection, air - sea interactions, midlatitude climate variability.

Submitted –November 2010.

Revised manuscript –February 2011.

*Author address: Dr. A. Czaja, Imperial College, Prince Consort Road, Huxley Building, Room 726; London SW7 2AZ, UK. tel: +44 (0)20 7594 1789 fax: +44 (0)20 7594 7900 email: a.czaja@imperial.ac.uk

Abstract

The role of moist convection in “transferring” upward surface ocean conditions throughout the troposphere is studied in reanalysis data for the Northern and Southern extra-tropical Hemispheres in winter. It is found that conditions for the development of a convective air column from the sea surface to the tropopause are met frequently over all major western boundary currents and their extension in the oceanic interior (sometimes by as much as 50% of the time). These large occurrences are shown to be jointly controlled by oceanic advection of warm waters and, on the atmospheric side, by the downward displacement of the tropopause associated with synoptic weather systems.

Based on these results, it is proposed that the oceans can influence the atmosphere directly through convection in midlatitudes, as is commonly thought to occur in the Tropics. Analysis of the Richardson number R_i found at low levels suggest that moist symmetric instability ($0 < R_i \leq 1$) is a key process involved in linking surface ocean temperatures to atmospheric lapse-rates, in addition to standard upright convection. These low R_i processes are not currently parameterized in climate models, which raises the possibility that the extra-tropical oceanic influence on climate might be underestimated in the current generation of models.

1 Introduction

The current generation of climate models shows a clear cut behavior regarding the role of ocean-atmosphere interactions in generating climate variability. On the one hand, the models need the interaction between the ocean and the atmosphere in order to simulate large scale climate variability in the Tropics (El Nino events). On the other hand, the dominant (annular) modes of extra-tropical climate variability do not owe their existence to such two-way interactions between the oceans and the atmosphere. They are found to behave realistically in atmosphere-only simulations, and the extra-tropical oceans seem to respond primarily passively to their time fluctuations (e.g., Czaja et al., 2003).

The response of atmospheric general circulation models (hereafter GCMs) to basin scale extra-tropical sea surface temperature (hereafter SST) anomalies has indeed shown to be elusive, sometimes appearing localized and baroclinic, sometimes appearing in the form of equivalent barotropic wavetrains. In their review of the subject, Kushnir et al. (2002), emphasized the complex dependence of the atmospheric GCMs response to details of the background mean flow and to details of the intrinsic low frequency variability of the model. More recently, however, global satellite observations of surface wind-stress and sea surface temperature have suggested a larger oceanic influence

on the atmosphere on spatial scale of $\simeq 100km$ in midlatitudes (e.g., Chelton et al., 2004), an impact possibly not limited to the atmospheric boundary layer but reaching to greater heights in the atmosphere (e.g., Minobe et al., 2008).

In this contribution, we investigate whether moist convective processes could be instrumental in coupling oceans and atmosphere in midlatitudes, as they are thought to be in the Tropics. This hypothesis is encouraged by the studies mentioned in the previous paragraph, but is also motivated by the recent suggestion that moist convection plays a role in setting the thermal stratification of the extra-tropical atmosphere (e.g., Jukes et al., 2000; Korty and Schneider, 2007; Pauluis et al., 2008). Korty and Schneider (2007) showed convincing evidence that neutrality to moist convection is often observed over the extra-tropical oceans in winter, and it is the purpose of this note to assess whether this observation allows to link surface ocean conditions to atmospheric lapse rates, maybe up to the tropopause level.

The note is structured as follows. In section 2, we introduce a conceptual model of a baroclinic wave and how, under certain conditions, it can develop a convective column from the sea surface to the tropopause. The occurrence of these conditions is then tested in the ERA interim data (Berrisford et al., 2009) in section 3. A discussion and a conclusion are offered in section 4 and 5, respectively.

2 Motivation: a criterion for the occurrence of deep (surface to tropopause) moist convection in midlatitude baroclinic waves

Undulations of the height of the tropopause are routinely observed in synoptic weather maps, travelling eastward around the globe in midlatitudes (e.g., Hoskins et al., 1985). When the tropopause is anomalously low, a positive tropospheric potential vorticity (PV) anomaly is created, reflecting the much higher values of PV in the stratosphere than in the troposphere. This PV anomaly induces cyclonic winds decaying towards the Earth's surface (e.g., Jukes, 1994), which, to the east of the displaced tropopause, advect poleward and upward warm and moist air from lower latitudes (Fig. 1).

A consequence of these motions is that the displaced subtropical air mass can become saturated and, if its entropy is larger than that of the air at the tropopause, this air mass can become convectively unstable. Indeed, a saturated atmosphere is unstable to vertical displacements when the (moist) buoyancy frequency $N_{moist}^2 < 0$, which occurs when specific entropy s de-

creases with height z (Emanuel, 1994)¹:

$$N_{moist}^2 = \Gamma_m \frac{\partial s}{\partial z} \quad (1)$$

(in this expression $\Gamma_m > 0$ is the moist adiabatic lapse-rate). To grow, the upper level cyclonic circulation must be coupled to a surface cyclone, but the latter must be to the east of the former (Eady, 1949). This leads, ahead of the depressed tropopause, to poleward advection at upper level and equatorward advection below (Fig. 1). When this happens near the western boundary of ocean basins, the low level air is of continental origin² and its advection over the warm ocean leads to large upward sensible and latent heat fluxes at the air-sea interface: as the upper air mass is brought to saturation, so is the low level air mass (so long as the moistening effect dominates over the rise in temperature in setting high relative humidity). If the entropies of air near the surface ocean boundary (s_{sb}), that of air near the tropopause (s_{tp}) and that of the midlevel subtropical air mass (s_{st}) satisfy $s_{tp} < s_{st} < s_{sb}$, a convective instability from the sea surface to the tropopause can occur.

The above idealized model suggests that when the previous inequali-

¹Small terms depending on the total water content were neglected in Emanuel's equation (6.2.10).

²An anonymous reviewer suggested that this state of affair is relevant to the Gulf Stream but less so to the Kuroshio extension. It is plausible that the ocean thermal front itself plays this role in the North Pacific.

ties are satisfied, sea surface temperature conditions can be communicated throughout the depth of the troposphere via moist convective processes. To test whether this occurs frequently or not in midlatitudes, a thermodynamic analysis of the ERA interim dataset is conducted next poleward of 20° in the Northern and Southern Hemispheres.

3 Application to the ERA interim dataset

3.1 Data and methods

The ERA interim dataset is a reanalysis of the global atmosphere covering the data-rich period since 1989, and continuing in real time (Berrisford et al., 2009). It uses 60 levels in the vertical and a spectral truncation of T255 (the reduced Gaussian grid has a $\simeq 79km$ spacing for surface and other grid-point fields). Even though this resolution is higher than that of most climate models, convection is still heavily parameterized, following the mass flux scheme of Tiedtke (1989). This situation is not ideal for our purpose, but has to be weighted against the large number of observations which constrain the model through time. Note that other studies have used reanalysis data with success to study the impact of extra-tropical moist convection on atmospheric dynamics (e.g., Korty and Schneider, 2007; Pauluis et al., 2008).

Daily (12.00 UTC) fields of temperature (T), specific humidity (q_v), water vapor pressure (e), total pressure P , total water content (q_T) and relative humidity (RH) were used to compute the specific entropy of moist air s according to (Emanuel, 1994):

$$s = (q_T c_l + (1 - q_T) c_{pd}) \ln \frac{T}{T_o} - R_d (1 - q_T) \ln \frac{(P - e)}{P_{do}} + q_v \frac{l_v}{T} - R_v q_v \ln RH \quad (2)$$

in which $T_o = 273.15K$ is a reference temperature, $P_{do} = 1000mb$ a reference pressure, c_l is the specific heat capacity of liquid water, c_{pv} that of water vapor at constant pressure, R_d and R_v are the gas constants for dry air and vapor, respectively, and l_v is the enthalpy of vaporization for water vapor, approximated as $l_v = l_v(T) = l_{vo} - (c_l - c_{pv})(T - T_o)$ with $l_{vo} = 2.5 \times 10^6 Jkg^{-1}$.

The tropopause was tracked as a surface of constant potential vorticity ($PV = 2PV$ -unit was chosen, following for example Hoskins et al., 1985). The entropy s_{tp} was estimated by first computing the values of T, P, e, q_v, q_T and RH along the 2 PV -unit surface and then using those values in (2).

The criterion developed in the preceding section ($s_{tp} < s_{st} < s_{sb}$) is not ideally suited to a direct application to observations. First, the calculation of s_{st} is not as straightforward as that of s_{tp} because it requires an estimate of the meridional scale of the parcel's displacement driven by a low tropopause event (or a Lagrangian trajectory calculation in order to track the exact origin and entropy of the subtropical air parcel "entrained" in the synoptic

system). In addition, even if it were satisfied somewhere in the atmosphere at a given time, the associated air column would quickly overturn and reach a nearly uniform entropy profile with height: put simply, unstable conditions are unlikely to be observed. An alternative to the previous inequalities could thus be to check for weak vertical entropy gradients, proceeding from the sea surface upward, but we opted instead for a simpler approach, which is to look for profiles satisfying $s_{tp} < s_o$ in which s_o is the entropy that an air parcel would have from (2) if (i) at the same temperature as the surface ocean (ii) at the pressure found at the sea surface and (iii) at a relative humidity of 80% (note that the SST from the ERA interim data is used for the calculation of s_o). The rationale for this choice is that s_o thus defined is an upper bound on the entropy possibly found at low levels³ and so satisfying $s_{tp} < s_o$ is a necessary condition for the convective events of the type described in section 2 to occur. We classify accordingly a gridpoint on a given daily map as *potentially* unstable to deep (surface to tropopause) moist convection if, at that gridpoint:

$$s_{tp} - s_o < 0 \tag{3}$$

³This is because low level air has a temperature lower than SST and a relative humidity below 80%. Only far from wintertime continental boundaries would this temperature and relative humidity be reached.

3.2 Results

The fraction of days where the criterion (3) is satisfied is shown for the Northern Hemisphere winter of 2003-04 (December through February) in Fig. 2a, and for the Southern Hemisphere winter of 2004 (June through August) in Fig. 2b. Over vast stretches of ocean it is seen that the criterion is only rarely met, typically less than 10 % of the time (note that both land and sea ice covered gridpoints are not considered in these plots). Over the western sides of ocean basin though, the situation is very different, with the fraction exceeding 50 % of the time in some locations.

Besides this western intensification, there are two very interesting features in Fig. 2 which need further discussion. First, although the largest values of s_o are found at low latitudes, where the SST is largest⁴, these regions are not those dominating in Fig. 2. The reason is that the tropopause's height is large (low pressure) with only weak time variations over these regions and, as a result, s_{tp} is systematically larger than s_o . Put differently, the key feature explaining Fig. 2 is the high occurrence of low tropopause events over the major storm - track systems: a low tropopause has low entropy because of the upward advection of low potential temperature surfaces below it (Hoskins et al., 1985). In a calculation in which s_{tp} is fixed to its wintertime mean

⁴The effect of surface pressure on s_o is weak.

value rather than varying daily, the large occurrences in Fig. 2 disappear (not shown).

The second interesting feature is the imprint of the ocean circulation. Rather than displaying a broad land - sea contrast type pattern, the maps in Fig. 2 capture the structure of the major western boundary current systems. This is particularly pronounced over the Gulf Stream, where the thin ribbon associated with advection of warm waters from lower latitudes is clearly visible in Fig. 2a. The ocean circulation's imprint is also seen in the asymmetry between high latitudes of the North Atlantic and the high latitudes of other ocean basins: in the North Pacific and the Southern ocean, the occurrences found in Fig. 2 do not exceed 10 % poleward of 50° of latitude whereas they reach 20 to 30% poleward of $50^\circ N$ in the North Atlantic. In a calculation in which SSTs are uniformly lowered by $2^\circ C$ in the North Atlantic (while keeping the same daily values of s_{tp}), occurrences drop below 10% in most of the Northwestern Atlantic (not shown). This suggests that the presence of the North Atlantic drift, and its associated transport of warm waters to high latitudes, is an important contributor to the high occurrences found in Fig. 2. The low occurrences found at high latitudes of the Southern Ocean show less sensitivity to uniform changes in SST: it would take a warming of at least $5^\circ C$ to increase the occurrences to 20 – 30% poleward of $50^\circ S$ (not shown).

To illustrate what happens on a given day where the criterion (3) is satisfied, meridional - height sections of entropy and vertical velocity are shown in Fig. 3a and b, respectively. The section chosen is along $55^\circ W$, a longitude at which $s_{tp} < s_o$ is satisfied at $40^\circ N$ for the day considered. The broad distribution of entropy shows the expected low values at high latitudes of each Hemisphere and high (and more uniform) values in the Tropics (Fig. 3a). At $40^\circ N$, entropy is nearly constant from the surface to the tropopause (indicated by the thick black line) and the relative humidity reaches 100 % throughout this layer (not shown), as envisioned in section 2. The occurrence of deep convection at $(55^\circ W, 40^\circ N)$ on that day is confirmed by an inspection of vertical velocities in Fig. 3b, which shows a meridionally narrow but vertically broad (from the surface to the tropopause, the latter being indicated by the thick black line on the figure) region of ascent at $40^\circ N$. The magnitude of the ascent is large, on the order of $1 Pa s^{-1}$ (about a thousand *mb* in one day), a value only matched at that longitude and time within the inter-tropical convergence zone a few degrees south of the equator.

More insight into the mechanisms involved when the convective potential is realized, as in Fig. 3, is provided in Fig. 4. The latter displays the probability distribution function of the Richardson number R_i computed at

700mb according to:

$$R_i \equiv \frac{N_{moist}^2}{|\partial \vec{U}_{700} / \partial z|^2} \quad (4)$$

in which $|\partial \vec{U}_{700} / \partial z|^2$ measures the vertical shear of the horizontal velocity vector at 700mb and N_{moist}^2 was introduced in (1). The calculation displayed in Fig. 4 was only carried out over the portion of the North Atlantic where the $s_{tp} - s_o < 0$ condition is met more than 25 % of the time and the surface-to-tropopause averaged relative humidity exceeds 80%. The distribution peaks at $R_i = 0$, characteristic of standard, upright convection, but another peak is found near $R_i = 1$, the critical value marking the onset of moist symmetric instability (or “slantwise” convection –see Bennetts and Hoskins, 1979; Emanuel, 1983a). The integrated distribution over the $0 < R_i \leq 1$ interval is twice as large as that corresponding to the peak centered at $R_i = 0$, suggesting that slantwise convection dominates the dynamics at low level. This result is in agreement with the analysis of Korty and Schneider (2007 –comparing their Figs. 9 and 10).

Finally, in order to link more explicitly atmospheric thermodynamic conditions near the sea surface to those at mid-to-upper levels over the Gulf Stream region, the density temperature⁵ of an air parcel lifted adiabatically

⁵The density temperature T_ρ of a sample of air is defined as $T_\rho = T(1 - q_T - q_v R_v / R_d)$, using the notations from section 3.1. At fixed pressure, T_ρ is inversely proportional to density and thus provides a measure of buoyancy (e.g., Emanuel, 1994).

and reversibly (i.e., without exchange of heat with the surroundings and conserving its total water content q_T and entropy s) from 950mb is compared to that of its environment over the 900mb – 300mb layer (Fig. 5). Each dot on the scatterplot indicates the result of the calculation on a given day, averaging on that day the thermodynamic properties over the region of the Gulf Stream where the condition $s_{tp} - s_o < 0$ is met more than 25% of the time. In addition, since low static stability is expected for low pressure systems only, a grid point of that region on that day was considered in the averaging only if its surface pressure was lower than its wintertime mean.

The black circles indicate the result of the calculation when the parcel is lifted vertically upward, thereby testing the stability of the air column to standard upright convection. It is seen that the environment is typically more buoyant than the parcel by a few degrees K , the circles falling to the right of the “moist neutral diagonal” (the $x = y$ curve shown as the black continuous line). As expected, the rms difference between the density temperature of the parcel and that of its environment increased when considering high pressure rather than low pressure systems (from 4.9K to 8.9K), but more interestingly, the correlation seen in Fig. 5 (black circles) also deteriorated as a result (not shown). This indicates more coherence between low and mid-to-upper levels in cyclones than anticyclones, and supports the idea that moist neutrality is approached in low pressure systems (e.g., Juckes, 2000).

The Richardson number analysis in Fig. 4 showed that slantwise convection, in addition to standard upright convection, is also involved in air-sea interactions near the Gulf Stream. The buoyancy calculation above was thus repeated for slanted, rather than upright, displacement of air parcels (gray circles in Fig. 5)⁶ The circles now fall even more closely onto the “moist neutral” diagonal, with the rms difference between the density temperature of the parcel and that of the environment being $3.1K$ instead of $4.9K$ in the upright case. Overall, the buoyancy calculation in Figure 5 suggests that low level ($950mb$) thermodynamic conditions over the Gulf Stream are indeed communicated over a deep layer ($900mb - 300mb$) via convective processes.

3.3 Discussion

The physical picture of a column convecting from the sea surface to the tropopause (section 2) is admittedly a crude representation of the complex mechanisms found in extra-tropical weather systems (e.g., Browning, 1986).

⁶Following Emanuel (1983b), the ascent was computed along a surface of constant angular momentum $M \equiv fx + v_T$ in which v_T is the velocity perpendicular to the thermal wind vector, f is the Coriolis parameter, and x is the distance in the direction perpendicular to the thermal wind vector. The latter was estimated as the average of the vertical shear at $700mb$ and at $400mb$. Note that the calculation was only performed when those two shear vectors differed by less than 10 degrees in direction in order to satisfy the assumption of two-dimensionality implicit in the theory of slantwise convection –see Emanuel (1983b).

Indeed, the latter move eastward and as they do so, entrain air masses of different geographical origins (e.g., Green et al., 1966). For the local picture adopted in this study to hold, the timescale for the convective processes must be less than the time taken for the system to cross the western boundary current regions. Inspection of daily maps of tropopause heights suggest that low tropopause anomalies take a couple of days to do so, consistent with an eastward extension of the western boundary current regions of about $\simeq 1000km$ and a system displacement velocity of $\simeq 10ms^{-1}$. This time is less than that of moist symmetric instability (on the order of the local inertial period $f^{-1} \simeq 3$ hours at $40^\circ N$ –see Emanuel, 1983a) and of standard upright convection (an hour or so). We thus suggest that the physical picture of section 2 is relevant to air-sea interactions near the western boundary current regions, a view clearly reinforced by the buoyancy calculation in Fig. 5.

If the convective potential $s_{tp} - s_o < 0$ was realized as frequently as depicted in Fig. 2, the troposphere would find itself under the direct influence of the ocean ($s \simeq s_o$ from the sea surface to the tropopause) for as much as 50 % of the time over the western boundary current regions in winter. Analysis of alternative criteria (column averaged relative humidity, vertical velocities) suggest however that the potential is only achieved about 10 % of the time (not shown), leaving to the ocean a one-week “window” to the

troposphere every winter. It is not clear at present what controls when the convective potential is realized and when it is not. The results of Korty and Schneider (2007) suggest that baroclinic waves are efficient at stratifying the 700 – 800 mb layer (see their Fig. 8c). This could prevent unstable conditions near the sea surface to develop further vertically, thereby providing an overall “break” on the mechanism schematized in Fig. 1. Further work is needed to test this hypothesis.

Finally, a striking feature of the analysis presented here is its emphasis on the western boundary current regions. This contrasts with the study by Korty and Schneider (2007) whose results showed western intensification at low levels but not aloft (their Fig. 9). A possible explanation could be the use of a fixed level analysis in Korty and Schneider (2007), while the analysis presented here follows the tropopause. However, after repeating the calculation of Fig. 2 using the entropy at 300 mb rather than at the tropopause, the same western intensification was found (not shown). It is more likely that the difference reflects the emphasis on surface conditions considered here (testing the stability of air columns to upward displacements from the sea surface) as opposed to conditions in the bulk of the atmosphere in Korty and Schneider (saturation PV in a given volume of air). In other words, a possible physical interpretation of the difference between this study and that of Korty and Schneider (2007), is that convection is rooted in the

boundary layer over western boundary current regions, while it is less so elsewhere. This is an interesting question which requires further work to be fully elucidated.

4 Conclusions

In this contribution we have investigated a mechanism by which the distribution of sea surface temperature can affect the extra-tropical atmosphere. The physical picture is simple and reminiscent of that often invoked in the Tropics, whereby oceanic temperature conditions are transmitted vertically up to the tropopause through moist convective processes. The introduction and analysis of a new measure of convective potential over the oceans shows that the wintertime occurrence of convectively neutral situations (i) can be found from the sea surface to the tropopause but the latter must be anomalously low (i.e., closer to the sea surface than on average) and (ii) is primarily found over western boundary current regions of the Southern and Northern Hemispheres, where advection of warm waters maintain a large thermodynamic imbalance with the atmosphere.

The convective mechanism is appealing because it bypasses the difficulties associated with wave mean flow interactions at the core of understanding how sea surface temperature conditions affect the atmospheric circulation in the

extra-tropics (Kushnir et al., 2002). It is however not clear at present how much of this “vertical influence” translates into a climatic influence away from the western boundary current regions. A possibility is that the occurrence of moist neutral conditions over the western boundary current regions helps maintain a high Eady growth rate there (i.e., low dry stratification), thereby being instrumental in setting the location of the storm-track. This line of thought was first proposed by Hoskins and Valdes (1990), who invoked the baroclinic response of the atmosphere to the diabatic heating associated with land - sea contrast, rather than moist neutrality. Hoskins and Valdes (1990) were not able to convincingly show a role for ocean currents, as the heat lost in winter by the oceans could be regained the following summer. Our results however clearly point towards ocean currents as the key ingredients allowing moist neutral condition to be achieved, as is evident from the oceanic dynamical structures in Fig. 2.

The importance of ocean currents and western boundary current regions found here is reminiscent of the recent study by Nakamura et al. (2008) –see also Booth et al. (2010). They proposed that air - sea heat exchanges at oceanic fronts are responsible for restoring the baroclinicity of the atmosphere at low levels. This mechanism of ocean-atmosphere coupling is complementary to the one discussed here in that it emphasizes the role of the ocean in restoring horizontal temperature gradients in the atmosphere at

low levels (their study), as opposed to restoring vertical temperature profiles to a moist adiabat over a deep tropospheric layer (this study).

Finally, it was found that moist symmetric instability (Richardson number of unity or less) was an important mechanism to “transmit” vertically oceanic conditions. This instability is not parameterized in the current generation of climate models, which suggests that the extra-tropical oceanic influence on climate, and its associated predictability, might currently be underestimated in climate models. This exciting prospect deserves further consideration.

Acknowledgements: N. Blunt was funded by a bursary from the Nuffield foundation. Discussions with B. Hoskins and R. Hide helped in focusing the ideas presented in this note. Comments from an anonymous reviewer and Rob Korty helped improve the manuscript.

References

- Bennetts, D. A., and B. J. Hoskins, 1979: Conditional symmetric instability - a possible explanation for frontal rainbands, *Quart. J. Roy. Met. Soc.*,105, 945-962.
- Berrisford, P., et al., 2009: The ERA interim archive, ERA Report series 1.
- Browning, K. A., 1986: Conceptual models of precipitating systems, *Weather and Forecasting*, 1, 23-41.
- Booth, J. F., L. Thompson, J. Patoux, K. A. Kelly and S. Dickinson, 2010: the signature of the midlatitude storm-track on the surface winds, *J. Clim.*, 23, 1160-1174.
- Chelton, D. B., et al., 2004: Satellite measurements reveal persistent small-scale Features in Ocean Winds, *Science*,303, 978-983.
- Czaja, A., A. W. Robertson, and T. Huck, 2003: The role of coupled processes in producing NAO variability, *Geophysical Monograph*, AGU, 134, 147-172.
- Eady, E. T., 1949: Long waves and cyclone waves, *Tellus*, 1, 33-52.
- Emanuel, K. A., 1983a: The lagrangian parcel dynamics of moist symmetric instability, *J. Atm. Sci.*, 40, 2368-2376.
- Emanuel, K. A., 1983b: On assessing local conditional symmetric

- instability using local soundings, *Mon. Wea. Rev.*, 11, 2016-2033.
- Emanuel, K. A., 1994: *Atmospheric convection*, Oxford University Press, 580pp.
- Green, J. S., F. H. Ludlam, and J. F. R. McIlveen, 1966: Isentropic relative flow analysis and the parcel theory, 92, 210-219.
- Hoskins, B. J., M. E. McIntyre, and A. W. Robertson, 1985: On the use and significance of isentropic potential vorticity maps, *Quart. J. Roy. Met. Soc.*, 111, 877-946.
- Hoskins, B. J., and P. J. Valdes, 1990: On the existence of storm-tracks, *J. Atm. Sci.*, 47, 1854-1864.
- Jukes, M. N., 1994: Quasigeostrophic dynamics of the tropopause, *J. Atm. Sci.*, 51, 2756- 2768.
- Jukes, M. N., 2000: The static stability of the midlatitude troposphere: the relevance of moisture, *J. Atm. Sci.*, 57, 3050-3057.
- Korty, R. L., and T. Schneider, 2007: A climatology of the tropospheric thermal stratification using saturation potential vorticity, *J. Clim.*, 20, 5977-5991.
- Kushnir, Y. et al., 2002: Atmospheric GCM response to extratropical SST anomalies: synthesis and evaluation, *J. Clim.*, 15, 2233-2256.
- Minobe, S., et al., 2008: Influence of the Gulf Stream in the troposphere, *Nature*, 452, 206-210.

-Nakamura, H, T. Sampe, A. Goto, W. Ohfuchi and S. Xie, 2008: On the importance of mid-latitude oceanic frontal zones for the mean state and dominant variability in the tropospheric circulation, *Geophys. Res. Let.*, 35, L15709, doi:10.1029/2008GL034010.

-Pauluis, O., A. Czaja and R. Korty, 2008: The global atmospheric circulation on moist isentropes, *Science*, 321, 1075-1078.

-Tiedtke, M., 1989: A comprehensive mass flux scheme for cumulus parameterization in large scale models, *Mon. Wea. rev.*, 117, 1779-1800.

List of Figures

- 1 Schematic of conditions possibly leading to surface-to-tropopause convection in a growing baroclinic wave. The tropopause is indicated by the dashed black line, while cyclonic circulations are depicted by the gray curvy arrows. At mid-to-upper levels, warm and moist air of subtropical origin is brought to saturation by poleward and upward advection (gray arrow). At low level, cold and dry air is brought to saturation by surface evaporation over the ocean (black arrow). The entropies s_{tp} (tropopause), s_{st} (subtropical) and s_{sb} (surface boundary) referred to in the text are also indicated. 26
- 2 Fraction of days (in percent) for which the criterion $s_{tp} - s_o < 0$ is met poleward of 20° for (a) the Northern winter of 2003-2004 and (b) the Southern hemisphere winter of 2004. The calculation was not carried out over continents (black) and sea ice (fraction of days set to zero) covered gridpoints. 27

- 3 Latitude - Pressure (in mb) sections at $55^\circ W$ on February 10th 2004 at 12.00 UTC. (a) specific entropy (in $Jkg^{-1}K^{-1}$, contoured every $25Jkg^{-1}K^{-1}$ for $s \leq 300Jkg^{-1}K^{-1}$ and $50Jkg^{-1}K^{-1}$ for $s \geq 300Jkg^{-1}K^{-1}$) and (b) pressure vertical velocity (in $Pa s^{-1}$, contoured every $0.5Pa s^{-1}$, continuous when negative, i.e. upwards). In both panels the tropopause location ($2PVU$ surface) is indicated by the thick black line. The black blocks indicate orography. 28
- 4 Probability distribution function of the Richardson number at $700mb$ over “moist” Gulf Stream profiles during the 2003-04 winter. See text for details. 29
- 5 Comparison of daily density temperatures (in K) averaged over the $900mb - 300mb$ layer ($\equiv \langle T_\rho \rangle$) for Gulf Stream cyclones during the 2003-04 winter. On the y -axis, $\langle T_\rho \rangle$ corresponds to the layer - averaged density temperature of a parcel lifted adiabatically and reversibly from $950mb$ (upright in black, slanted in gray). On the x -axis, the actual $\langle T_\rho \rangle$ is given. See text for details. 30

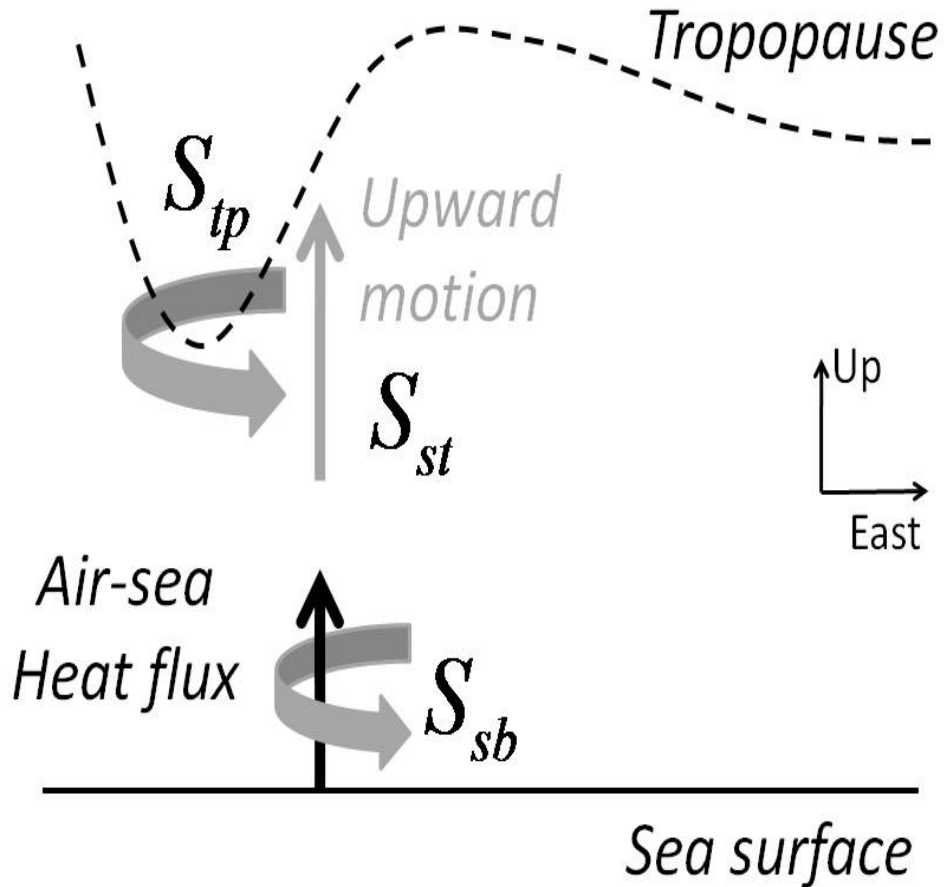


Figure 1: Schematic of conditions possibly leading to surface-to-tropopause convection in a growing baroclinic wave. The tropopause is indicated by the dashed black line, while cyclonic circulations are depicted by the gray curly arrows. At mid-to-upper levels, warm and moist air of subtropical origin is brought to saturation by poleward and upward advection (gray arrow). At low level, cold and dry air is brought to saturation by surface evaporation over the ocean (black arrow). The entropies s_{tp} (tropopause), s_{st} (subtropical) and s_{sb} (surface boundary) referred to in the text are also indicated.

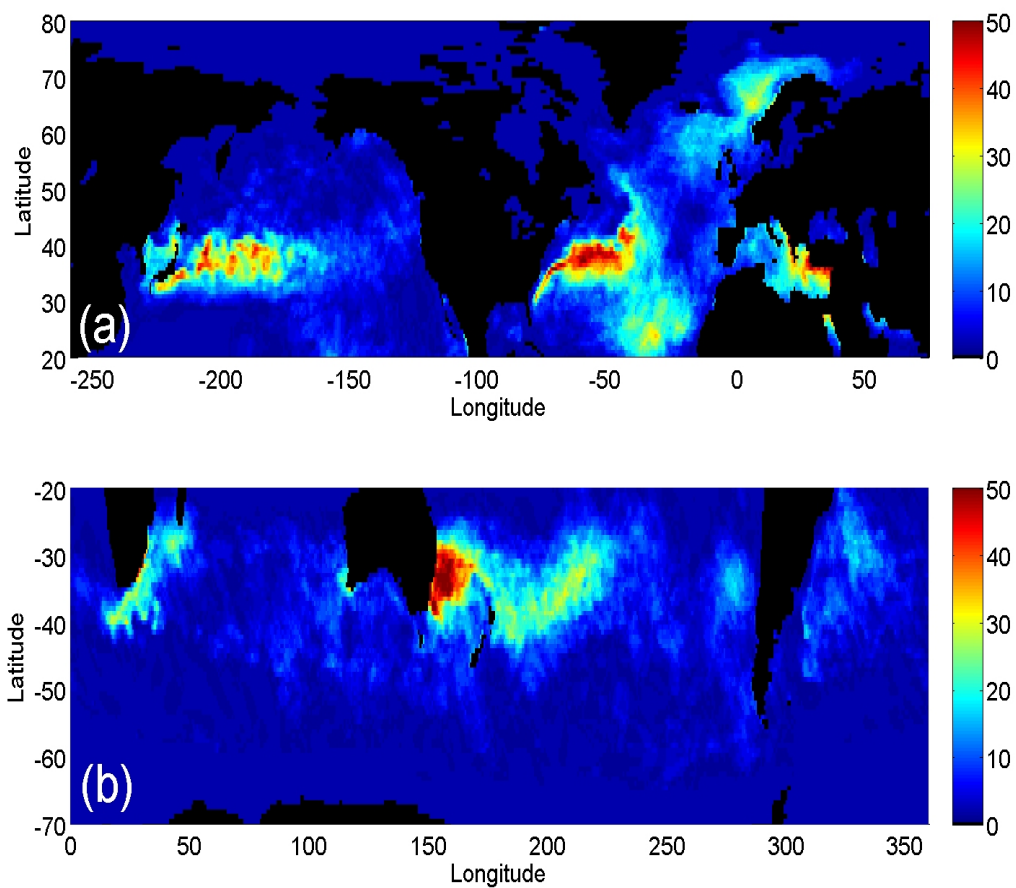


Figure 2: Fraction of days (in percent) for which the criterion $s_{tp} - s_o < 0$ is met poleward of 20° for (a) the Northern winter of 2003-2004 and (b) the Southern hemisphere winter of 2004. The calculation was not carried out over continents (black) and sea ice (fraction of days set to zero) covered gridpoints.

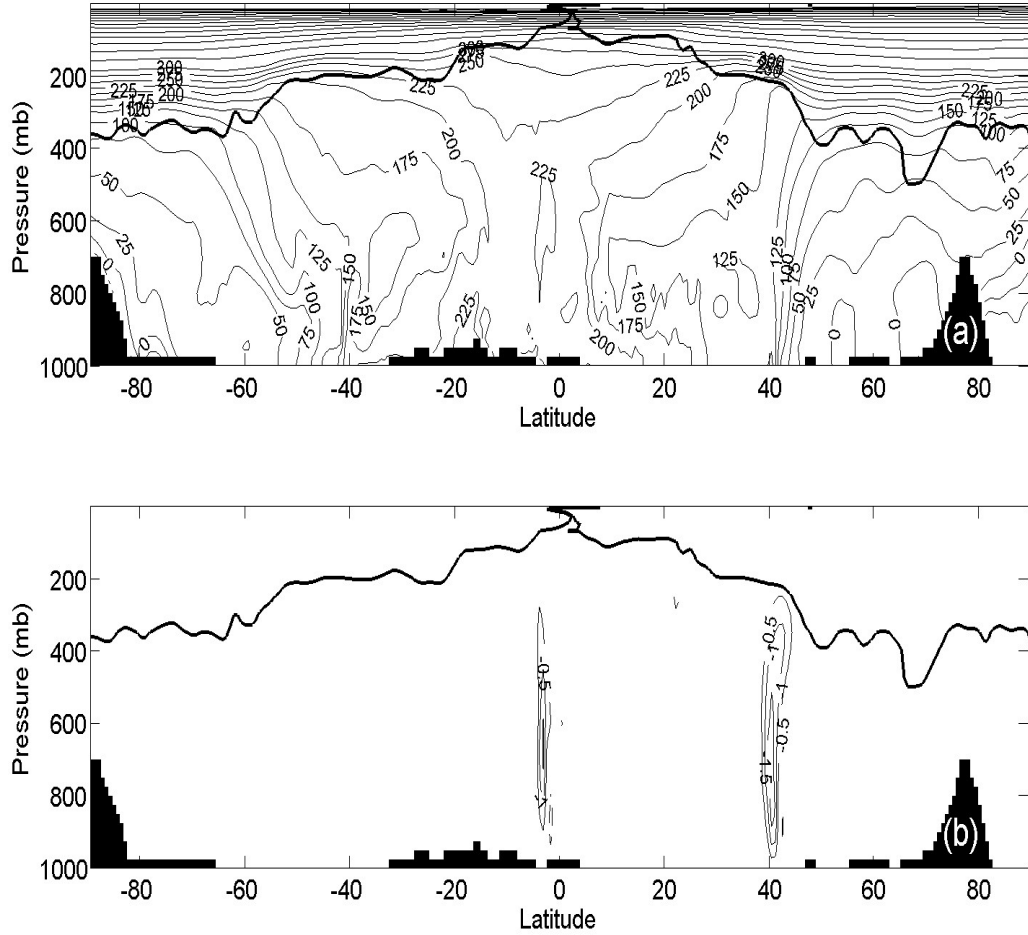


Figure 3: Latitude - Pressure (in mb) sections at $55^{\circ}W$ on February 10th 2004 at 12.00 UTC. (a) specific entropy (in $Jkg^{-1}K^{-1}$, contoured every $25Jkg^{-1}K^{-1}$ for $s \leq 300Jkg^{-1}K^{-1}$ and $50Jkg^{-1}K^{-1}$ for $s \geq 300Jkg^{-1}K^{-1}$) and (b) pressure vertical velocity (in Pas^{-1} , contoured every $0.5Pas^{-1}$, continuous when negative, i.e. upwards). In both panels the tropopause location ($2PVU$ surface) is indicated by the thick black line. The black blocks indicate orography.

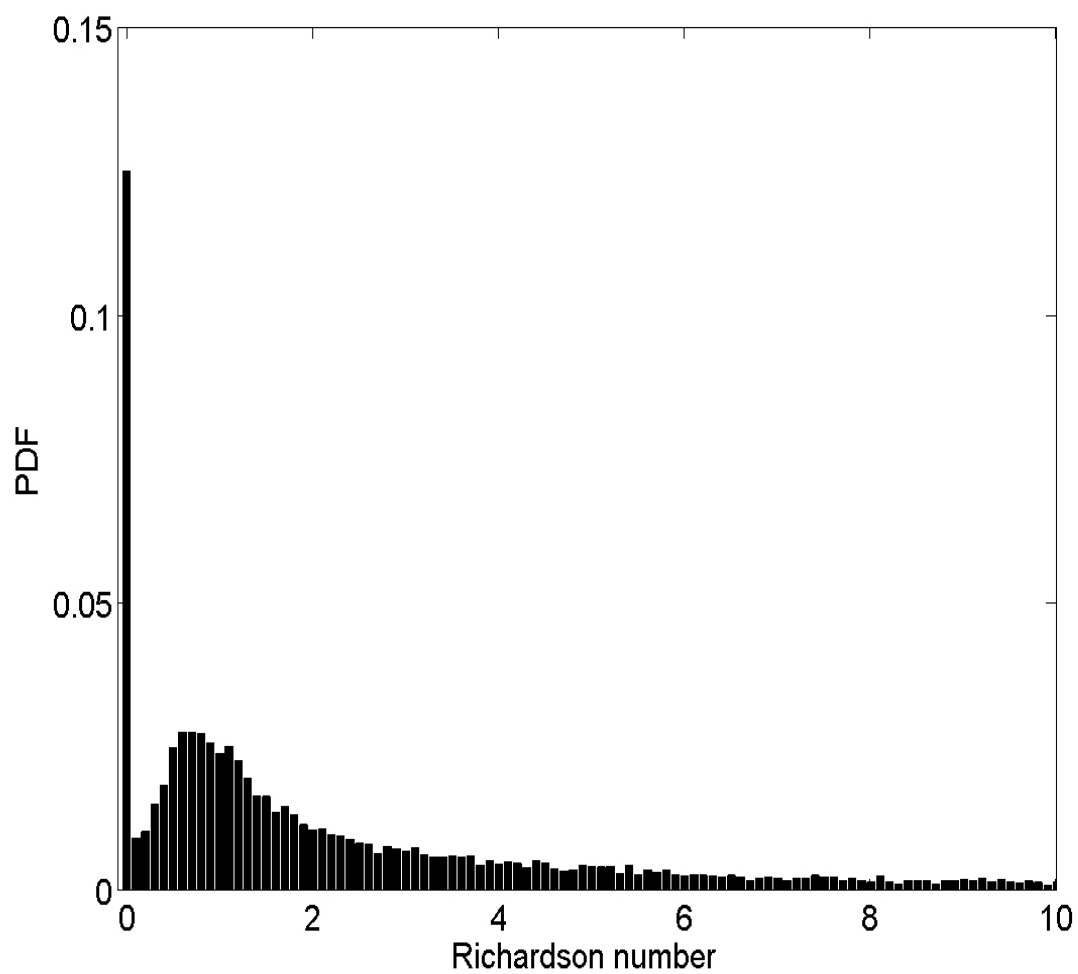


Figure 4: Probability distribution function of the Richardson number at $700mb$ over “moist” Gulf Stream profiles during the 2003-04 winter. See text for details.

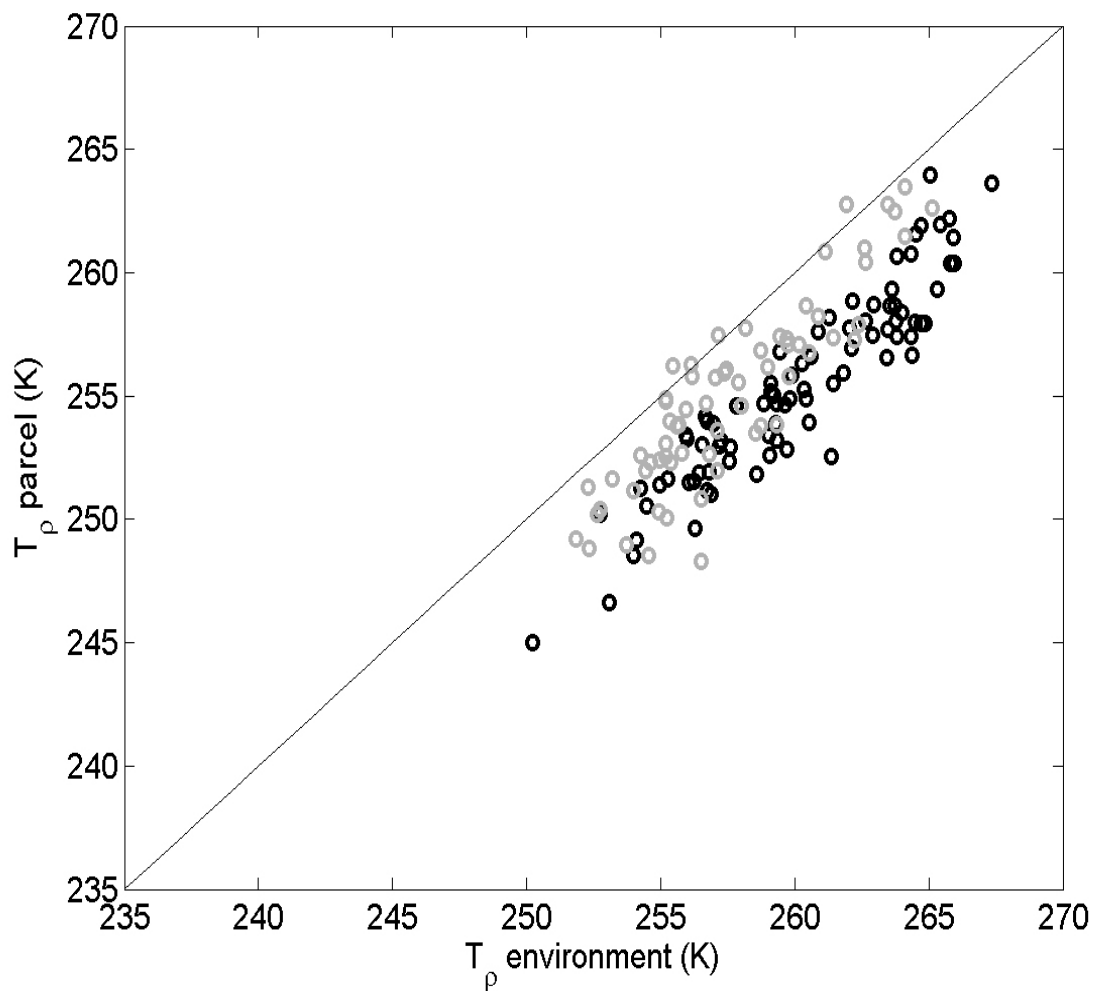


Figure 5: Comparison of daily density temperatures (in K) averaged over the $900mb - 300mb$ layer ($\equiv \langle T_\rho \rangle$) for Gulf Stream cyclones during the 2003-04 winter. On the y -axis, $\langle T_\rho \rangle$ corresponds to the layer - averaged density temperature of a parcel lifted adiabatically and reversibly from $950mb$ (upright in black, slanted in gray). On the x -axis, the actual $\langle T_\rho \rangle$ is given. See text for details.